Biomath Forum

Biomath Communications

www.biomathforum.org/biomath/index.php/conference

Mathematical modeling of bioprocesses with the use of fractional order derivatives

Vladimira Suvandjieva
Sofia University "St. Kliment Ohridski"
valdi_h@abv.bg

Supervisor:
Ivan Bazhlekov

Citation: Vladimira Suvandjieva, Mathematical modeling of bioprocesses with the use of fractional order derivatives, Biomath Communications 8, pp. 1-48, https://doi.org/10.11145/bmc.2021.04.017

Abstract

This work brings together two recently discussed topics: mathematical modeling of a bioreactor and working with derivatives of non-integer order. Generally, it turns out that it is reasonable to replace the integer order derivatives in some of the already well known mathematical models describing bioprocesses with fractional order ones. However, the specific structure of such type of derivatives makes the study of the properties of the models a real challenge. This work contains primary results for modeling of a bioreactor with appropriately selected numerical approximations. Different scenarios are taken into consideration: starting from the simplest one – without mortality and then complicating by adding nonzero mortality term. In the classical case the solution of the system of differential equations describing the process has a specific behaviour in terms of monotonicity. Therefore, the focus of the further examinations is to find out whether it is possible to generalize the model into a fractional order one such that the key properties considering monotonicity still hold. The results show that the latter requires certain dependencies between the orders of the derivatives in the mathematical model. The hypothesis is based on two types of experiments which are described in detail. Lotka-Volterra and Monod specific growth rate are used in the mathematical model. The paper contains figures which illustrate the results from different numerical computations performed via Wolfram Mathematica software.

Keywords: Bioprocess; Bioreactor; specific growth; Explicit Euler method; Diffusion; Fractional order derivative; Rieman-Liouville fractional order derivative; Caputo fractional order derivative; Adams-Bashforth-Moulton method; Mortality rate; Lotka-Volterra model; Monod model

Contents

1 Introduction

Fractional calculus is that part of calculus where fractional order integral and differential operators and their properties and applications are studied. It is still considered to be new and innovative topic despite some significant mathematicians such as Riemann, Liouville and Caputo had been researching it. Fractional calculus increases interest with its applications in physics, engineering and biological processes [Diethelm, 2016]. The motivation for many classical mathematical models being modified into fractional order derivative ones is the opportunity for obtaining better, in terms of quantity, results – closer to the provided experimental ones [Toledo-Hernandez, Rico-Ramirez, Iglesias-Silva, and M.Diwekar, 2014] and many recently conducted numerical experiments confirm it [Diethelm, 2016, Bazhlekov and Bazhlekova, a]. An important property of the fractional order derivative models, unlike the classical ones, is the *memory effect* [Diethelm, 2016]. It is caused by the non-local structure of the fractional order derivatives and is essential for the modeling of biological processes.
On the other hand, still little is known about the quality properties of the fractional order derivative models. In contrast to the classical models where the analytical examination of properties such as, for example, monotonicity, is well adopted through the years and is nowadays no difficulty to work with, the analytical approach of fractional order derivative models turns out to be a great challenge. The information about the properties of a mathematical model is important for deciding whether the model is suitable for describing of a given model.

The focus of this thesis is the usage of fractional order derivatives in the mathematical modeling of bioprocesses. Certain models are examined and the numerical results are presented. Some basic theoretical facts about fractional order derivatives are exposed in section 2. There are given the Riemann-Liouville and the Caputo definitions for fractional order derivative, also some important properties, similarities and differences between of them. The next section 3 consists of

the description of the mathematical model (and its main components) which will be the subject of the following numerical investigations. The general form of the model is given. First, the classical model and some of its alternatives (different specific growth rate) are considered in section 4. Important analytical properties are obtained in the case of Lotka-Volterra model. Those properties are supported by the numerical results for Lotka-Volterra, Monod, Haldane, Andrews and Webb specific growth rate. For that purpose explicit Euler method is used. Section 5 focuses on the modeling of a simplified version of the adsorption process in two-phase fluid system by adding a diffusion term to one of the equations constituting the classical model. The obtained results for different values of the diffusion constant are attached in this section. The generalization of the classical model into fractional order derivative one is given in section 6. Dependencies between the orders of the derivatives in the model for which the monotonicity remains the same as for the classical model are detected via appropriately selected numerical procedure. Similar research about the qualitative behaviour of the solution is performed for the fractional order derivative model when a mortality rate is included in section 7. Section 8 summarizes the main results and discusses possibilities for future investigations.

2 Fractional order derivatives. Definitions and properties

By the term "fractional order derivative" or just "fractional derivative" is meant, as it is clear from the name, derivative of non-integer order. Many definitions for a fractional derivative exist nowadays [Samko, Kilbas, and Marichev, 1993, Kilbas, Srivastava, and Trujillo, 2006]. Two of the most popular ones – the Riemann-Liouville and the Caputo definition [Gorenflo and Mainardi, 1997] are considered here.

According to the Riemann-Liuoville approach to the fractional calculus, it is natural to define a fractional integral of order $\alpha > 0$ of

function $f(t)$ as a generalization of the Cauchy's formula:

$$J^n f(t) := \frac{1}{(n-1)!}\int_0^t (t-\tau)^{n-1} f(\tau) d\tau, t > 0 \tag{1}$$

where n is a positive integer.
For the transition from integer values of the index to fractional ones in a natural way, the Gamma function is needed. Actually, considering that $(n-1)! = \Gamma(n)$, one can simply define integral of order $\alpha > 0$ with the following equality:

$$J^\alpha f(t) := \frac{1}{\Gamma(\alpha)}\int_0^t (t-\tau)^{\alpha-1} f(\tau) d\tau, t > 0 \tag{2}$$

with $J^0 := I$ where I is the identity operator.
Here are some easily obtained properties:
1. The semi-group property:

$$J^\alpha J^\beta = J^{\alpha+\beta} \tag{3}$$

2. Commutativity (follows from 1.):

$$J^\alpha J^\beta = J^\beta J^\alpha \tag{4}$$

3. Effect on power functions:

$$J^\alpha t^\gamma = \frac{\Gamma(\gamma+1)}{\Gamma(\gamma+1+\alpha)} t^{\alpha+\gamma}, \alpha > 0, \gamma > -1, t > 0. \tag{5}$$

2.1 Riemann-Liouville definition

From here on D^n denotes the n^{th} derivative operator where n is a positive integer. The following holds:

$$D^n J^n = I, \tag{6}$$

$$J^n D^n \neq I \tag{7}$$

and furthermore (from (1))

$$J^n D^n f(t) = f(t) - \sum_{k=0}^{n-1} f^{(k)}(0^+) \frac{t^k}{k!}. \tag{8}$$

It is natural from the definition of D^α for $\alpha \in \mathbf{R}^+$ to be required that

$$D^\alpha J^\alpha = I \tag{9}$$

which leads to the following definition:
Definition 1: *(Riemann-Liouville derivative of order $\alpha > 0$)*

$$D^\alpha f(t) := \begin{cases} \frac{d^m}{dt^m}\left[\frac{1}{\Gamma(m-\alpha)} \int_0^t \frac{f(\tau)}{(t-\tau)^{\alpha+1-m}} d\tau\right], & m-1 < \alpha < m \\ \frac{d^m}{dt^m} f(t), & \alpha = m \end{cases} \tag{10}$$

or briefly,

$$D^\alpha f(t) := D^m J^{m-\alpha} f(t), \tag{11}$$

where m is such a positive integer for which:

$$m - 1 < \alpha \leq m,$$

i.e. $m = \lceil \alpha \rceil$. For completeness is defined $D^0 = J^0 = I$.
The following equality holds (similar to the integer option (6)):

$$D^\alpha J^\alpha = I, \forall \alpha > 0. \tag{12}$$

Indeed,

$$D^\alpha J^\alpha = D^m J^{m-\alpha} J^\alpha = D^m J^{m-\alpha+\alpha} = D^m J^m = I,$$

where (11), the semi-group property (3) and a common property of the integer order derivatives (6) are sequentially applied in order to get the latter.
It is essential to be mentioned that, unlike the integer order case, if $\alpha \notin \mathbf{N}$, $D^\alpha 1 \neq 0$ (and hence $D^\alpha const \neq 0$):

$$D^\alpha 1 = D^m J^{m-\alpha} 1 = D^m\left(\frac{1}{\Gamma(m-\alpha)} \int_0^t (t-\tau)^{m-\alpha-1} t\tau\right) = \frac{1}{\Gamma(m-\alpha)} D^m \frac{t^{m-\alpha}}{m-\alpha}$$
$$= \frac{1}{\Gamma(m-\alpha)} \frac{t^{-\alpha}(m-\alpha)(m-\alpha-1)...(1-\alpha)}{m-\alpha} = \frac{t^{-\alpha}}{\Gamma(1-\alpha)}.$$

The last equality in the sequence follows from the recurrent dependence

$$\Gamma(z) = \frac{\Gamma(n+z+1)}{z(z+1)...(z+n)}, z+n>0, n \in N \tag{13}$$

after replacing $z = 1-\alpha$ and $n = m-1$.
Note: *The poles of Gamma function are 0,-1,-2,..., and hence* $\frac{t^{-\alpha}}{\Gamma(1-\alpha)} \neq 0, \forall \alpha \notin \mathbf{N}$.

2.2 Caputo definition

Definition 2: *(Caputo derivative of order* $\alpha > 0$*)*

$$D_*^\alpha f(t) := \begin{cases} \frac{1}{\Gamma(m-\alpha)} \int_0^t \frac{f^{(m)}(\tau)}{(t-\tau)^{\alpha+1-m}} d\tau, & m-1 < \alpha < m \\ \frac{d^m}{dt^m} f(t), & \alpha = m \end{cases} \tag{14}$$

or briefly,

$$D_*^\alpha f(t) := J^{m-\alpha} D^m f(t), \tag{15}$$

where again $m = \lceil \alpha \rceil$. The first main difference between the Caputo fractional derivative and the Riemann-Liouville one is the fact that the Caputo definition for fractional order derivative requires absolute integrability of the derivative of order m.
It is easy to obtain

$$D^\alpha f(t) := D^m J^{m-\alpha} f(t) \neq J^{m-\alpha} D^m f(t) =: D_*^\alpha f(t), \tag{16}$$

based on the fact that

$$D^\alpha f(t) = D_*^\alpha f(t) + \sum_{k=0}^{m-1} \frac{t^{k-\alpha}}{\Gamma(k-\alpha+1)} f^{(k)}(0^+). \tag{17}$$

A property similar to (8) (the integral of derivative property) can be obtained in the sense of the Caputo definition:

$$\begin{aligned} J^\alpha D_*^\alpha f(t) &= J^\alpha J^{m-\alpha} D^m f(t) = J^{\alpha+m-\alpha} D^m f(t) \\ &= J^m D^m f(t) = f(t) - \sum_{k=0}^{m-1} f^{(k)}(0^+) \frac{t^k}{k!}. \end{aligned}$$

Note: *One can prove the latter property when using consistently the semi-group property (3) and property (8).*
The integral of derivative property leads to the fact that solving Caputo fractional order derivative equations requires initial data for the unknown function and its integer-order derivatives. This makes the Caputo derivative more suitable for applications unlike the Riemann-Liouville derivative where the integral of derivative expression contains integro-differential operators of the unknown function at $t = 0$. Because of that only Caputo fractional order derivatives in the interval $(0, 1)$ are used here. In this case, $m = 1$ and integral of Caputo derivative equals $f(t) - f(0)$. This means that only the initial value $f(0)$ of the unknown function $f(t)$ will be necessary for solving the corresponding mathematical model.
Another signifficant property of the Caputo derivative which distinguishes it from the Riemann-Liouville derivative is:

$$D_*^\alpha const \equiv 0. \tag{18}$$

The latter follows immediately from the definition of the Caputo fractional derivative (15) as it is firstly applied integer order derivative of constant which is identical with 0.

3 Mathematical model

The focus here is the modeling of a bioreactor [Diethelm, 2016, Bazhlekov and Bazhlekova, a, Alt and Markov, 2012]. Bioreactors are used for the production of bio-fuel (e.g. biodiesel and bioethanol), biological surfactants, etc. Generally, the bioreactor is a container full of some material – the so called substrate (usually some sugar such as fructose or glucose), biomass (bacteria), and also some other components which will be considered insignificant for the process and hence are not taken into account in the mathematical model. As a result of the bioprocess a bioproduct is produced. The general form

of the problem is represented by the following system:

$$\begin{cases} D_*^{\beta} b(t) = \mu(s(t))b(t) - mb(t),\ 0 < t \leq T \\ D_*^{\sigma} s(t) = -k\mu(s(t))b(t),\ 0 < t \leq T \\ D_*^{\epsilon} e(t) = p\mu(s(t))b(t),\ 0 < t \leq T \\ b(0) = b_0,\ s(0) = s_0,\ e(0) = 0,\ 1 \geq \beta > 0,\ 1 \geq \sigma > 0,\ 1 \geq \epsilon > 0 \end{cases} \tag{19}$$

$b(t)$ – biomass
$s(t)$ – substrate
$e(t)$ – ethanol
$\mu(s(t))$ – specific growth rate
m – mortality coefficient
k, p – other parameters.

Note: *The function $\mu(s) \geq 0$ is defined for $s \geq 0$ and may take various forms [Alt and Markov, 2012]. However, the main results in this work are obtained with Lotka-Volterra and Monod specific growth rate.*

A significant fact that should be mentioned is that the first two equations of (19) are independent from the third one. Hence, the general approach to the problem is to split into two sub-problems: first to solve the system of the first two equations (with the corresponding initial conditions). After that to solve the third equation with substituting the resulting solution $(b(t), s(t))$.

In the literature there exist different possibilities for the specific growth rate. The main focus here is the monotonicity of the solution of system (19). In the classical case ($\beta = \sigma = \epsilon = 1$) when mortality is not considered ($m = 0$), the analytical results (section 4, subsection 4.1) show monotonic behaviour of the model which is logical a biological point of view. The challenge is to observe whether these properties hold in the case when at least one of the values of the derivative orders in the model (19) is in the interval $(0, 1)$. In the classical case with mortality when $\beta = \sigma = 1$ some analytical results for the solution of (19) are obtained in section 7. Again the goal is to find out for which values of β and σ in the interval $(0, 1)$ those properties remain valid. Unfortunately, no matter what the value of m is, retrieving information about the properties of the analytical solution of (19) in the

fractional order derivative case seems unbearable for now. Therefore the further investigations require numerical approach. The primary results of this work show that there are indeed certain dependencies between the values of β, σ and ϵ in the interval $(0, 1)$ for which the monotonicity properties of the classical model still hold. It is encouraging that similar results are independently obtained in other works [Bazhlekov and Bazhlekova, a].

4 Classical model without mortality

$\beta = \sigma = \epsilon = 1$ and $m = 0$ is considered. Results for different specific growth rate parameters of the model are presented.

4.1 Lotka-Volterra model. Analytical properties

Important analytical results for the exact solution of (20) in the classical case without mortality (i.e. when $\beta = \sigma = \epsilon = 1$ and $m = 0$) are the topic of this subsection [Diethelm, 2016]. For that purpose Lotka-Volterra specific growth rate is used. Lotka-Volterra specific growth rate is a linear function $\mu(s) := cs$ where c is a positive constant. When the respective substitution of $\mu(s)$ in (19) is done, the following mathematical model of a bioreactor is obtained:

$$\begin{cases} D_*^{\beta} b(t) = cs(t)b(t) - mb(t) \\ D_*^{\sigma} s(t) = -kcs(t)b(t) \\ D_*^{\epsilon} e(t) = pcs(t)b(t) \\ b(0) = b_0,\ s(0) = s_0,\ e(0) = e_0. \end{cases} \tag{20}$$

Proposition 1. *In the case when $\beta = \sigma = \epsilon = 1$ and $m = 0$ there exists $T' > 0$ for which the system (20) has a unique solution in the interval $(0, T']$.*

Furthermore, one can assume that considering the positivity of the initial values b_0 and s_0 then from continuity follows that there is a

neighbourhood of 0 where $s(t)$ and $b(t)$ take positive values. The positivity of the solution of the problem is extremely important from a biological point of view considering the processes that are being modeled. Negative values for whichever one of the three unknown functions makes no sense and leads to the conclusion that the chosen model is inappropriate. To define the neighbourhood of 0, or briefly the interval $(0, T]$ where $b(t)$ and $s(t)$ take positive values, T is chosen as follows: $T := min\{T', B', S'\}$ where $B' := sup\{t \in (0, T) : b(\tau) > 0, \forall \tau \in (0, t)\}$ and $S' := sup\{t \in (0, T) : s(\tau) > 0, \forall \tau \in (0, t)\}$. Then the following statement holds:

Proposition 2: *In the case when $\beta = \sigma = \epsilon = 1$ and $m = 0$ there exists $T > 0$ such that the system (20) has a unique solution in the interval $(0, T]$, and $b(t) > 0, s(t) > 0, e(t) > 0, \forall t \in (0, T)$.*

Proof: *The positivity of $b(t)$ and $s(t)$ follows from the definition of T, while the positivity of $e(t)$ follows from the third equation of the system, namely: considering that $b(t) > 0, s(t) > 0, \forall t \in (0, T)$ and also the fact that p is a positive constant, then $\frac{de(t)}{dt} > 0, \forall t \in (0, T)$ which basically means that $e(t)$ is increasing on the interval $(0, T)$ and hence $e(t) > e(0) = 0, \forall t \in (0, T)$.* $\square$

Finally, based on these two propositions, the following theorem is formulated:

Theorem 1: *Under the conditions of* ***Proposition 1*** *and* ***Proposition 2*** *the following hold on the interval $(0, T)$:*

(a) *s is strictly decreasing,*

(b) *b and e are strictly increasing.*

Proof: *As already proven in* ***Proposition 2*** *$b(t) > 0, s(t) > 0, \forall t \in (0, T)$. Then from the positivity of the parameters k and p the following holds: $s'(t) < 0, b'(t) > 0, e'(t) > 0, \forall t \in (0, T)$ which is basically equivalent to* ***(a)*** *and* ***(b)****.* $\square$

The numerical experiments confirm that those analytical results hold not only for Lotka-Volterra model but for every other function $\mu(s)$ defining specific growth rate (figures 2, 3 and 4).

4.2 Monod model

One of the most common functions for modeling microbial growth is Monod function. It is defined as follows:

$$\mu_M(s) := \mu^* \frac{s}{K+s}, \tag{21}$$

where μ^* and K are positive constants. In the classical case ($\beta = \sigma = \epsilon = 1$) the problem (19) yields the following form (Monod model):

$$\begin{cases} \frac{db(t)}{dt} = \mu^* \frac{s(t)}{K+s(t)} b(t), \ 0 < t \leq T \\ \frac{ds(t)}{dt} = -k\mu^* \frac{s(t)}{K+s(t)} b(t), \ 0 < t \leq T \\ \frac{de(t)}{dt} = p\mu^* \frac{s(t)}{K+s(t)} b(t), \ 0 < t \leq T \\ b(0) = b_0, \ s(0) = s_0, \ e(0) = e_0. \end{cases} \tag{22}$$

Two sets of parameters of the model (22) are used for the numerical simulations:

$$\begin{aligned} &\mu^* = 0.09[h^{-1}], \ K = 68[ppm], \ k = 5, \ p = 10, \\ &b_0 = 100[ppm], \ s_0 = 200[ppm], \ e_0 = 0[ppm] \end{aligned} \tag{23}$$

and

$$\begin{aligned} &\mu^* = 0.6[h^{-1}], \ K = 0.81[g/L], \ k = 4.5, \ p = 3.4, \\ &b_0 = 0.1[g/L], \ s_0 = 5[g/L], \ e_0 = 0[g/L]. \end{aligned} \tag{24}$$

Note: *These parameters are experimentally established [Bandyopadhyay, Chowdhury, Bhattacharjee, and Pan, 2013], [Das, Calay, and Chowdhury, 2020] and the numerical results are attached respectively to [Bazhlekov and Bazhlekova, b] and [Bazhlekov and Bazhlekova, a]. It should be mentioned that the measuring units for the concentration are different in both sets. The unit used in (23) is particle per million [ppm] and the unit used in (24) is gram per liter [g/L]. The connection between both units is:* $1g/L = 1000ppm$. *In order to facilitate the comparison of the results obtained here with those in the corresponding publications, the measuring units in (23) and (24) are kept in their original form.*

For achieving comparability between the numerical results the experiments in this sections are performed with parameters (23) for Monod model and

$$c = 10^{-3}, k = 5, p = 10, b_0 = 100[ppm], s_0 = 200[ppm], e_0 = 0[ppm] \quad (25)$$

for Lotka-Volterra model. Figure 1 shows the similarity between the solutions of both models and an appropriate choice of parameters (25). The numerical results in this section are obtained by using explicit Euler method.

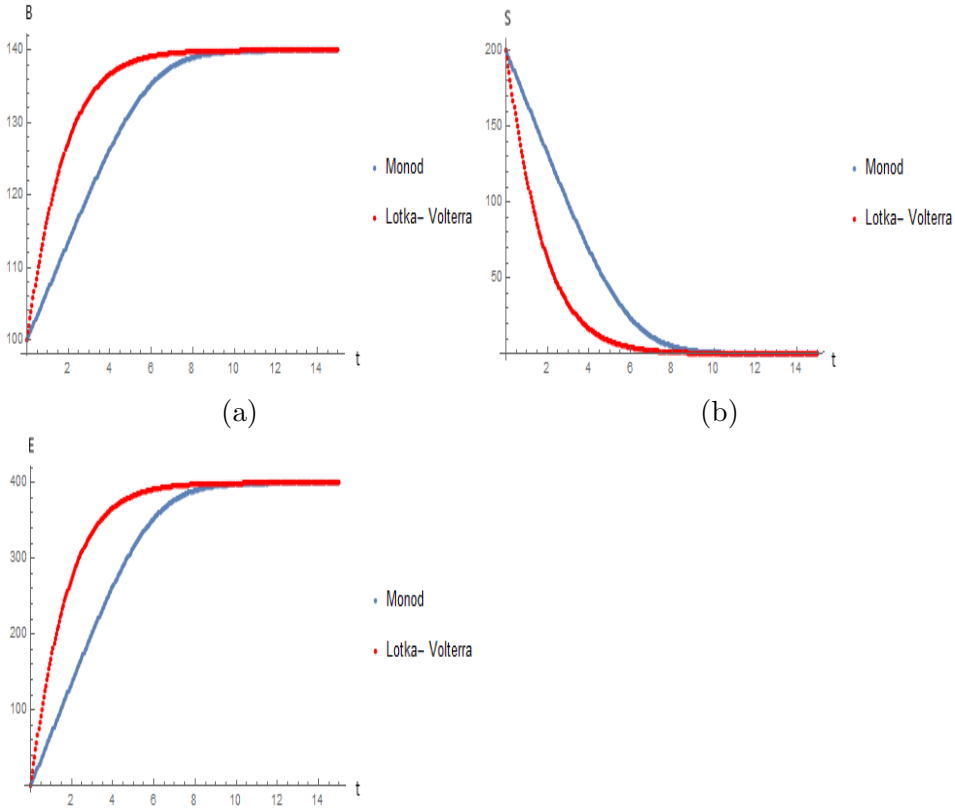

Figure 1: Graphs for the approximate solution B – (a), S – (b) and E – (c). Explicit Euler method at time step $\tau = 0.05$ is used for Lotka-Volterra and Monod model.

4.3 Alternatives of the specific growth rate

Some other popular functions describing microbial growth are [Alt and Markov, 2012]:
Webb:

$$\mu_W(s) := \mu^* \frac{s(1+\gamma\frac{s}{K_i})}{K+s+\frac{s^2}{K_i}}, \tag{26}$$

Haldane:

$$\mu_H(s) := \mu^* \frac{s}{(K+s)(1+\frac{s}{K_i})}, \tag{27}$$

Andrews:

$$\mu_A(s) := \mu^* \frac{s}{K+s+\frac{s^2}{K_i}}. \tag{28}$$

The corresponding mathematical models are not considered in detail, because at a proper choice of the parameters K_i and γ:

$$K_i = 680[ppm],\ \gamma = 0.65. \tag{29}$$

the numerical results do not significantly differ from those with Monod model, supposed the same initial conditions are used. This is illustrated in figures 3 and 4, where the numerical solutions of the model with different specific growth rate functions (26) – (28) are used for both sets of parameters (23) and (24) respectively. It is seen from the figures that the difference between the results for the different models are minor and for parameters (24) they are almost identical (figure 4).

4.4 Explicit Euler numerical method

As already mentioned in section 1, for the numerical solution of (22) the explicit Euler method is implemented. A comparison between the explicit and the implicit Euler method shows insignificant difference between the approximate solutions obtained by using both methods. Furthermore, considering the nonlinearity of the model, the implicit Euler method is much slower than the explicit one because at each iteration over time a nonlinear system of three equations has to be solved. Therefore, the explicit Euler method is chosen here.

First, a uniform mesh over the time interval $[0, T]$ with step τ is defined:

$$\omega_\tau := \{j\tau,\ j = 0, ..., m,\ m = \frac{T}{\tau}\}. \tag{30}$$

In the explicit Euler method for (22) the solution at time step j+1 is given by:

$$\begin{cases} B_{j+1} = B_j + \tau\mu^* \frac{S_j}{K+S_j} B_j,\ j = 0, ..., m-1 \\ S_{j+1} = S_j - \tau k\mu^* \frac{S_j}{K+S_j} B_j,\ j = 0, ..., m-1 \\ E_{j+1} = E_j + \tau p\mu^* \frac{S_j}{K+S_j} B_j,\ j = 0, ..., m-1 \\ B_0 = b_0,\ S_0 = s_0,\ E_0 = e_0, \end{cases} \tag{31}$$

where (B, S, E) is the approximate solution of the system (22).The local approximation error of this method is $O(\tau)$. The results for parameters (23) are given in figures 2a, 2b and 2c.
There exists exact solution of the system of differential equations

$$\begin{cases} \frac{db(t)}{dt} = \mu^* \frac{s(t)}{K+s(t)} b(t) \\ \frac{ds(t)}{dt} = -k\mu^* \frac{s(t)}{K+s(t)} b(t) \end{cases} \tag{32}$$

and it is given in [Alt and Markov, 2012] by an implicit function containing parameters which depend on the initial data. Hence using that result for solving Cauchy problem (22) is practically impossible. For this reason as a basis of comparison the numerical solution obtained using the built-in method NDSolve of the software Wolfram Mathematica is used. This solution is accurate enough in order to be used for determining the error of explicit Euler method (31). As already mentioned above, the local error of approximation is of order τ – the time step. Applying the explicit Euler method (31) with $\tau = 0.1; 0.01; 0.001; 0.0001$ and comparing the numerical solution with the respective one from applying NDSolve confirms that.

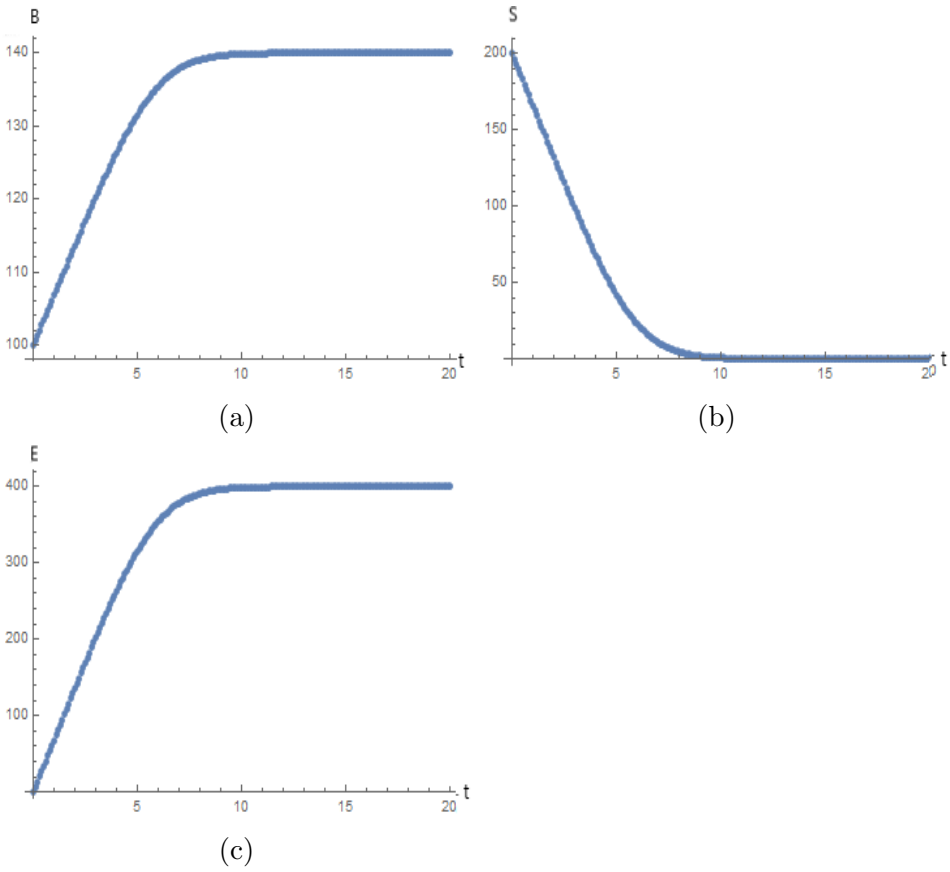

Figure 2: Graphs for the approximate solution B – (a), S – (b) and E – (c). Explicit Euler method at time step $\tau = 0.1$ is used for Monod model and parameters (23).

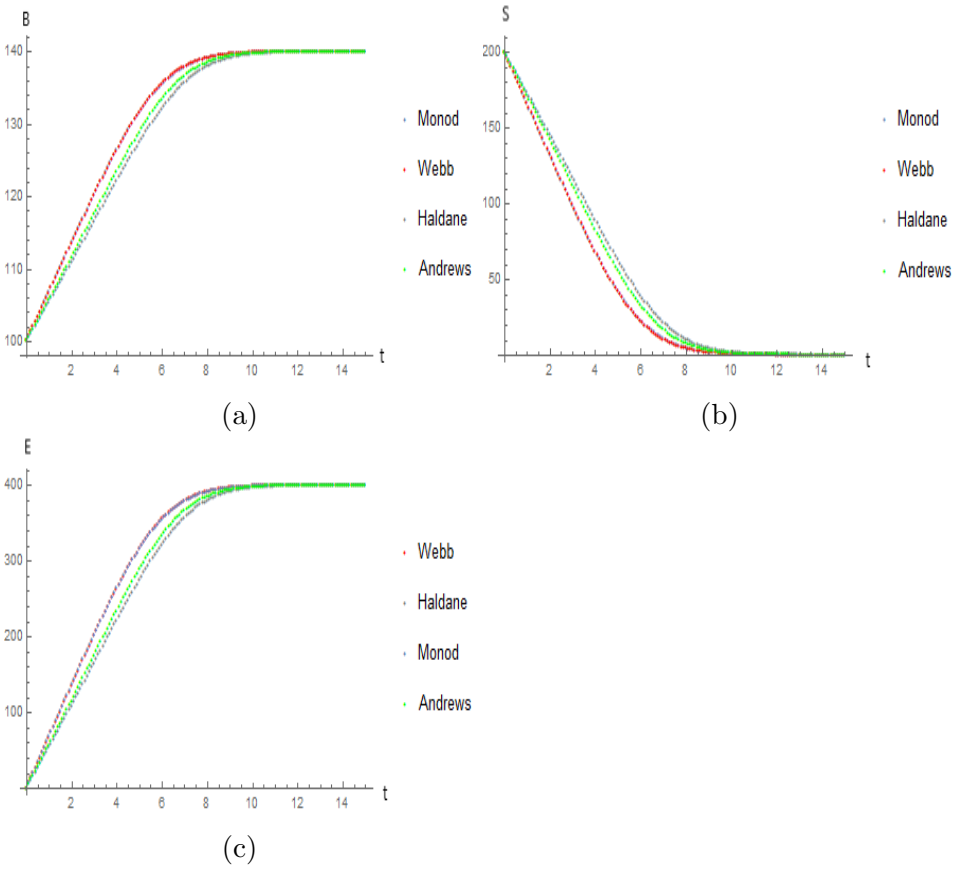

Figure 3: Graphs for the approximate solution B – (a), S – (b) and E – (c). Explicit Euler method at time step $\tau = 0.1$ is used for Monod, Haldane, Andrews and Webb model and parameters (23).

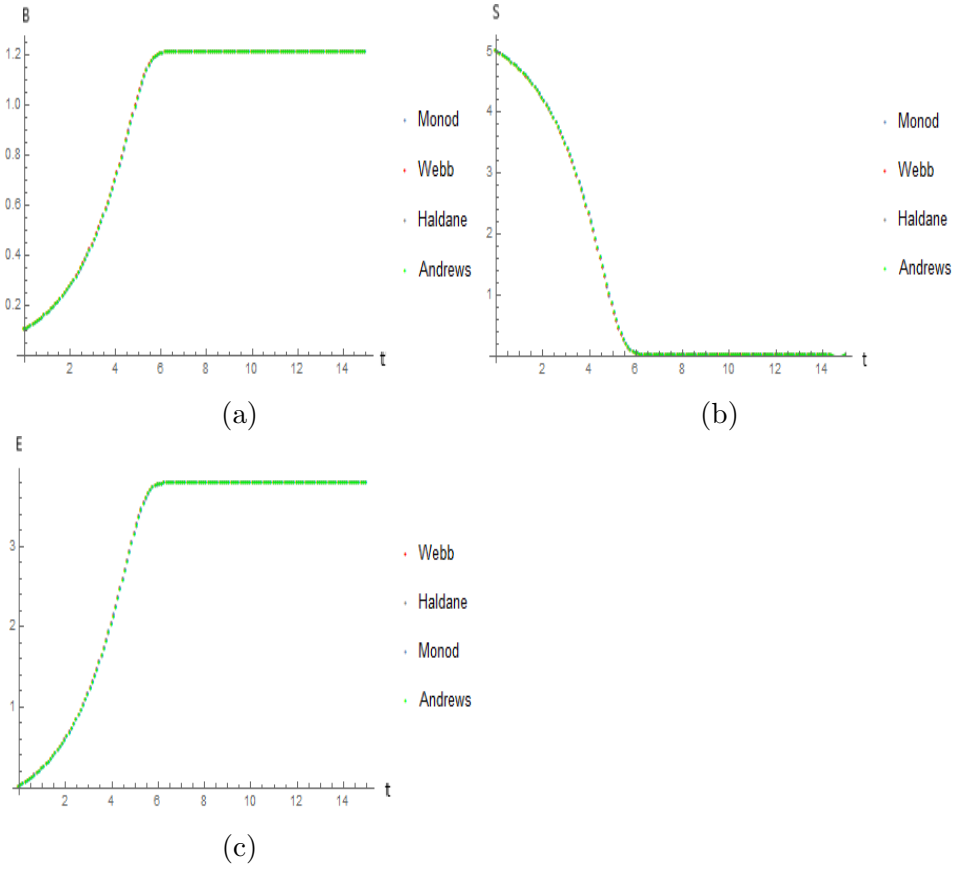

Figure 4: Graphs for the approximate solution B – (a), S – (b) and E – (c). Explicit Euler method at time step $\tau = 0.1$ is used for Monod, Haldane, Andrews and Webb model and parameters (24).

5 Model with diffusion

The subject of this section is a space dependent form of the process, i.e. when it depends not only from time but also from space. Such situation arises as a result of bioprocess in a two-phase fluid system. The substrate and the biomass are soluble only in one of the phases where the process occurs. The bioproduct, on the other hand, is soluble in both phases and/or is adsorbed at the interface. As a consequence of this transition there is a decrease of the bioproduct concentration on the interface which leads to unhomogeneous distribution of the bioproduct [Bazhlekov and Bazhlekova, b]. Here one-dimensional model is considered, which corresponds to adsorption on a flat interface. As the substrate (s) and the biomass (b) are homogeneously distributed, i.e. are space independent, the first two equations from (19) remain unchanged, while in the third one there is an additional diffusion term representing the flux due to unhomogeneous distribution of the bioproduct:

$$\begin{cases} \frac{db(t)}{dt} = \mu(s(t))b(t),\ 0 < t \leq T \\ \frac{ds(t)}{dt} = -k\mu(s(t))b(t),\ 0 < t \leq T \\ \frac{\partial e(t,x)}{\partial t} = d\frac{\partial^2 e(t,x)}{\partial x^2} + p\mu(s(t))b(t),\ 0 < t \leq T,\ 0 < x < X \end{cases} \tag{33}$$

with initial conditions

$$\begin{cases} b(0) = b_0 \\ s(0) = s_0 \\ e(0,x) = e_0,\ 0 < x < X \end{cases} \tag{34}$$

and boundary conditions

$$\begin{cases} e(t,0) = e_0,\ 0 < t \leq T \\ \frac{\partial e(t,x)}{\partial x}(t,X) = 0,\ 0 < t \leq T. \end{cases} \tag{35}$$

Note: *The choice of the first boundary condition is done in order to simply represent a model of adsorption at the interface where the*

concentration of the bioproduct is kept constant e_0*. The second boundary condition in this case is selected in order to express zero flux at a distance X from the interface.*
The focus of this section is on the initial-boundary problem (33) – (35) when $\mu_M(s) := \mu^* \frac{s(t)}{K+s(t)}$, i.e. Monod function.
It is well known that the smaller the diffusion coefficient $d > 0$ is, the "steeper" the graph of $e(t_1, x)$ is for small values of x (i.e. close to the inter-phase boundary) at any fixed time t_1. To illustrate this fact, several experiments for different values of d are performed. The values of the parameters of the bioprocess are again (23) and (24). As the first two equations do not depend on the third one, the approximate solutions for the substrate (S) and the biomass (B) remain the same as for the space independent model (figures 3a, 3b, 4a and 4b) and therefore only graphs of the approximate solution for the bioproduct (E) is presented.

The following explicit numerical method is implemented for the numerical solving of the initial-boundary value problem (33) – (35): A uniform mesh in time and space is defined:
$\omega_{h,\tau} := \omega_h \times \omega_\tau$, where
$\omega_h := \{ih,\ i = 0, ..., N,\ N = \frac{X}{h}\}$ and
$\omega_\tau := \{j\tau,\ j = 0, ..., M,\ M = \frac{T}{\tau}\}$.
As already mentioned above, the independence of the first two equations in (33) from the third one provides the opportunity for the following (explicit) two-part numerical method to be implemented:
1. In the first part the system of the first two equations of (33) with the corresponding initial conditions is solved numerically with the explicit Euler method (as already described in subsection 4.4
2. The already obtained approximate solution for the biomass $B = \{B_j,\ j = 0, ..., M\}$ and the substrate $S = \{S_j,\ j = 0, ..., M\}$ is then substituted in the third equation in order to find the approximate solution for the bioproduct $E = \{E_i^j,\ i = 0, ..., N,\ j = 0, ..., M\}$. Thus, the numerical procedure is as follows:

2.1 Determining the initial time layer according to (34):

$$E_i^0 = e_0,\ i = 0, ..., N \tag{36}$$

2.2 Determining the $j+1$-th time layer for $j = 0, ..., M-1$:

$$E_0^{j+1} = e_0, \tag{37}$$

$$E_i^{j+1} = \frac{d\tau}{h^2} E_{i-1}^j + (1 - 2\frac{d\tau}{h^2}) E_i^j + \frac{d\tau}{h^2} E_{i+1}^j + \tau p \mu(S_j) B_j,\ i = 1, ..., N-1, \tag{38}$$

$$E_N^{j+1} = 2\frac{d\tau}{h^2} E_{N-1}^j + (1 - 2\frac{d\tau}{h^2}) E_N^j + \tau p \mu(S_j) B_j. \tag{39}$$

Equations (37) and (39) correspond to the boundary conditions (35). To ensure stability of the numerical method described above, a condition for the positivity of its coefficients must be imposed. The only coefficient that is not necessarily positive is $1 - 2\frac{d\tau}{h^2}$ (equations (38) and (39)). Hence, the stability of the numerical method requires the following relationship between the steps over time and space:

$$\tau < \frac{h^2}{2d}. \tag{40}$$

Considering values of $d \in (0, 1]$ the condition (40) is satisfied if, for example, $\tau = \frac{h^2}{4}$. The numerical results from the above described method applied to (33) – (35) and different values of d are illustrated by figure 5.

The results presented in both figures 5a and 5b show that there is a boundary layer around the interface ($x = 0$), where concentration of the bioproduct E has significant gradient. Far from the interface (e.g. $x > 5$) concentration is practically space independent. It is also seen that the thickness of the boundary layer depends on the value of the diffusion coefficient d. Comparisons between concentration profiles for a given value of d presented in figures 5a and 5b indicate that the thickness of the boundary layer is almost insensitive on the values of the parameters of the bioreaction (i.e. (23) and (24)).

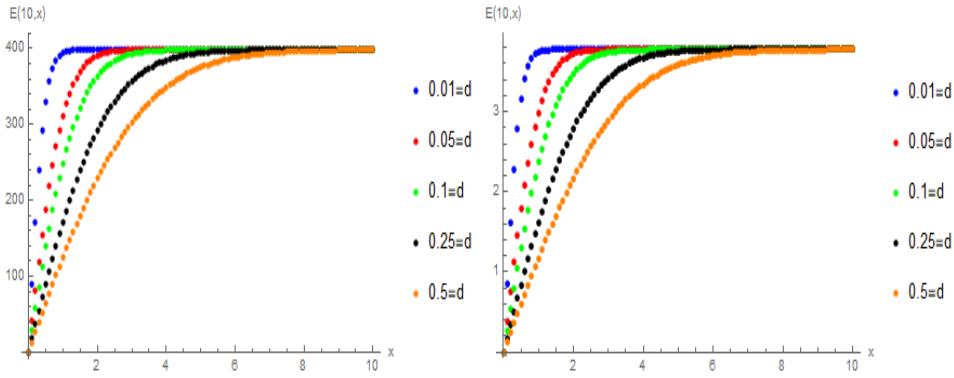

(a) (b)

Figure 5: Graphs for the approximate solution of E for $t = 10$ and $x \in (0, 10]$. The explicit method described in this section at time step $\tau = 0.1$ and $h = 0.0025$ is used for Monod model and parameters (23) – (a) and parameters (24) – (b). The diffusion coefficient d takes different values in the interval $(0, 1]$.

6 Fractional order derivative model

The classical model (with integer order derivatives), presented in section 4 is extended in the present section to the fractional order derivative model. In the case of the bioreactor problem, generally described with (19), this means that the values of the derivative orders β, σ and ϵ can be in the interval $(0, 1]$. As already mentioned in the beginning of this thesis, using time fractional order derivatives is really beneficial for modelling biological processes. The reason is in a particular property due to the non-local structure of the fractional order derivatives. The advantage of this property is its dependence from previous time interval (as its name suggests) which is essential for bioprocesses. On the contrary, using classical models provides only information about the current data which in many occasions can be misleading in terms of the relevant interpretation of the process. Unfortunately, the lack of analytical approach for the fractional analysis can lead to some significant difficulties for determining important qual-

itative properties (e.g. monotonicity) of the solution of the fractional derivative models. For the problem considered in this work, the property monotonicity is essential in terms of the accuracy of the model from a biological point of view: it is logical to expect that the substrate $s(t)$ is a decreasing function which tends to zero (for sufficiently long time). The biomass $b(t)$ (when no mortality is considered) and the bioproduct $e(t)$ are increasing in some interval $(0, T)$. In this section the model (19) is considered in the case of absence of mortality of the biomass ($m = 0$).

6.1 General form of the fractional order derivative model. A predictor-corrector numerical method

Before the numerical results for the concrete problem being exposed, the general form of the implemented for that purpose numerical method is briefly described. The case of fractional order derivative models requires the numerical solving of integral equations. This makes a significant difference with the common methods for numerical solving of differential equations. For the purpose of this work a predictor-corrector scheme of Adams type – The Adams-Bashforth-Moulton method is used. It can be applied for both linear and nonlinear problems, as well as to be extended for multidimensional equations [Baleanu, Diethelm, Scalas, and Trujillo, 2012, Diethelm, Ford, and Freed, 2002]. Consider the general form of the fractional order n-dimensional derivative problem:

$$\left\{ D_*^{\alpha} \mathbf{y}(t) = \mathbf{f}(\mathbf{y}(t)),\ 0 < t \leq T, \right. \tag{41}$$

with initial data

$$\mathbf{y}(0) = \mathbf{y}_0, \tag{42}$$

where $\alpha = (\alpha_1, ..., \alpha_n)$, $\alpha_i > 0, i = 1, ..., n$, $\mathbf{y}(t) = (y_1(t), ..., y_n(t))$, $\mathbf{f}(\mathbf{y}) = (f_1(\mathbf{y}), ..., f_n(\mathbf{y}))$ for some $n \in \mathbf{N}$. If $\alpha_i \in (0, 1]$ the problem

(41) is equivalent to the following Volterra integral equation:

$$\mathbf{y}(t) = \mathbf{y}(0) + \frac{1}{\Gamma(\alpha)} \int_0^t (t-\tau)^{\alpha-1} \mathbf{f}(\tau, \mathbf{y}(\tau)) d\tau. \tag{43}$$

Note: *For obtaining (43) both sides of (41) are integrated. After that the integral of derivative property given in subsection 2.2 is applied.*
For the implementation of the Adams-Bashforth-Moulton predictor-corrector method the uniform mesh (30) is used. The non-local structure of the fractional order derivatives (or the fact that in equation (43) there is integration from 0 to t) requires certain modifications of the classical Adams-Bashforth-Moulton predictor-corrector method of order 2 which is used in the classical model case (i.e. when $\alpha_i = 1, i = 1, ..., n$. There is a brief description of the method ($\mathbf{Y}$ denotes the approximate solution of (41) – (42)):
1. Setting the initial values (42):

$$\mathbf{Y}_0 = \mathbf{y}_0 \tag{44}$$

2. Calculation of the $k+1$-th approximation for $k = 0, ..., M-1$ via the following consecutive steps:
2.1 Finding the $k+1$-th predictor:

$$\mathbf{Y}^P_{k+1} = \mathbf{Y}_0 + \frac{1}{\Gamma(\alpha)} \sum_{j=0}^{k} \mathbf{b}_{j,k+1} \mathbf{f}(t_j, \mathbf{Y}_j) \tag{45}$$

2.2 Finding the $k+1$-th corrector:

$$\mathbf{Y}_{k+1} = \mathbf{Y}_0 + \frac{1}{\Gamma\alpha} (\sum_{j=0}^{k} \mathbf{a}_{j,k+1} \mathbf{f}(t_j, \mathbf{Y}_j) + \mathbf{a}_{k+1,k+1} \mathbf{f}(t_{k+1}, \mathbf{Y}^P_{k+1})), \tag{46}$$

where

$$\mathbf{b}_{j,k+1} := \frac{\tau^\alpha}{\alpha} ((k+1-j)^\alpha - (k-j)^\alpha), \tag{47}$$

$$\mathbf{A}^{k+1}_j := \begin{cases} k^{\alpha+1} - (k-\alpha)k^\alpha, \ j = 0 \\ (k-j+2)^{\alpha+1} - 2(k-j+1)^{\alpha+1} + (k-j)^{\alpha+1}, \ 1 \le j \le k \\ 1, \ j = k+1 \end{cases} \tag{48}$$

and

$$\mathbf{a}_{j,k+1} := \frac{\tau^{\alpha}}{\alpha(\alpha+1)}\mathbf{A}_{j,k+1}. \tag{49}$$

The method is described in more detail in [Diethelm, Ford, and Freed, 2002]. It can be proven that the order of this method is $O(\tau^p)$ where $p = min\{2, 1+\alpha\}$, or in other words, p is the minimum of the order of the corrector (which is 2) and the order of the predictor, which is 1 plus the order of the differential operator. As for its stability properties, they are at least as good as the corresponding properties of the respective Adams-Bashforth-Moulton predictor-corrector method of order 2 for the classical case [Diethelm, Ford, and Freed, 2002].

6.2 Monotonicity in the fractional order derivative case – propositions

After obtaining essential for the qualitative properties of the classical model results (subsection 4.1), it is logical to ask whether analogous of them can be obtained in the case when at least one of the values of β, σ, ϵ is not an integer, in the interval $(0, 1)$, to be more precise. It turns out that in this case an analytical approach still does not exist. Therefore, the focus of the work is with the help of appropriately selected numerical methods, to find out requirements for the values of $\beta, \sigma, \epsilon \in (0, 1]$ which guarantee the satisfaction of the qualitative properties of the classical model (monotonicity, in particular). A significant number of numerical experiments in this direction leads to the following conclusion:
(a) *For $\sigma \leq \beta$ b is increasing and for $\sigma > \beta$ b is not increasing for at least one set of parameters of the model,*
(b) *For $\sigma \leq \epsilon$ e is increasing and for $\sigma > \epsilon$ e is not increasing for at least one set of parameters of the model.*
The results for Lotka-Volterra and Monod model are presented in the next subsection.

To confirm the hypothesis about the dependencies between the values of β, σ and ϵ required for the maintenance of the monotonicity properties of the solution (i.e. the results from **Theorem 1**) two main

experiments are conducted.

First experiment: The purpose of this experiment is to examine the behaviour of the solution of the model for different values of β, σ and ϵ when two of them are fixed and the third one takes different values in the interval $(0, 1]$ and see in which cases B and E are monotonic. Here is how the experiment is set:

The system (19) with $m = 0$ is numerically solved with Adams-Bashforth-Moulton method. β, σ and ϵ are taken as parameters in the implementation of the method. Therefore these values are set manually for each calculation. The graphs of the solution B, S and E, respectively, are united for the different values of the non-fixed parameter (figures 6, 7, 8).

Second experiment: Unlikely the **First experiment** this one does not show the graphs of the approximate solution of the system (19) although it is been solved. The purpose of this experiment is to determine whether B and E are monotonic for a certain β, σ, ϵ and interval of time T. Here it is easier to investigate the behaviour of the solution for many different values of the parameters providing information only for its monotonicity – again unlikely the **First experiment**. Depending on which one will be investigated – B or E – there are two types of numerical calculations that can be made in this experiment:

(a) *For given (σ, β) to determine if B is increasing for the specified interval of time,*

(b) *For given (σ, ϵ) to determine if E is increasing for the specified interval of time.*

Both methods work on the same principle: for initialized (σ, β) (for **(a)**) and (σ, ϵ) (for **(b)**, $\beta = 1$ **is fixed**), first,

- The first two equations from (19) with $m = 0$ and the corresponding initial values are solved with the Adams-Bashforth-Moulton method - method **(a)**
- The whole system (19) with $m = 0$ is solved with the Adams-Bashforth-Moulton method – method **(b)**.

Then a counter is initialized at 0. For $j = 0, ..., M - 1$ if

- $B_{j+1} > B_j$ – method **(a)**
- $E_{j+1} > E_j$ – method **(b)**,

the counter increases with 1. This means that when the check is done for each $j = 0, ..., M-1$ the solution (B or E) is monotonic in the interval T only if the counter equals M. The result from both **(a)** and **(b)** is boolean: if the counter equals M at the end of the check, then the program returns 1, otherwise it returns 0. Graphically, this result is represented by a point in a coordinate system
- (σ, β) for **(a)** (figure 9a),
- (σ, ϵ) for **(b)** (figure 9b)
by multiplying the corresponding coordinates with the result from the experiment, i.e. 0 or 1. Thus, the point with these coordinates ((σ, β) or (σ, ϵ)) appears on the graph only if the solution (B or E) is monotonic in the interval $(0, T)$.

6.3 Numerical results for Lotka-Volterra and Monod model

Numerical results from **First experiment** and **Second experiment**, described in the previous subsection, for Lotka-Volterra and Monod model are presented here.

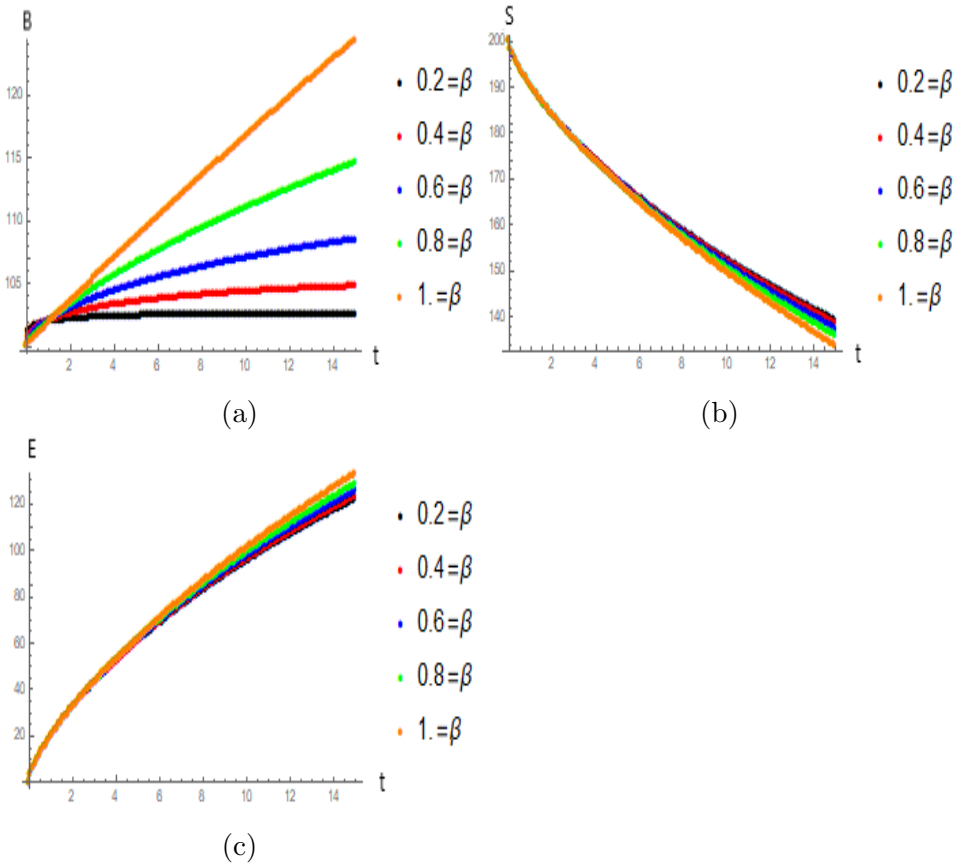

Figure 6: Graphs for the approximate solution B – (a), S – (b) and E – (c). Adams-Bashforth-Moulton method at time step $\tau = 0.1$ is used for Lotka-Volterra model and parameters (25). $\sigma = 0.75$, $\epsilon = 0.75$ and β takes different values in the interval $(0, 1]$.

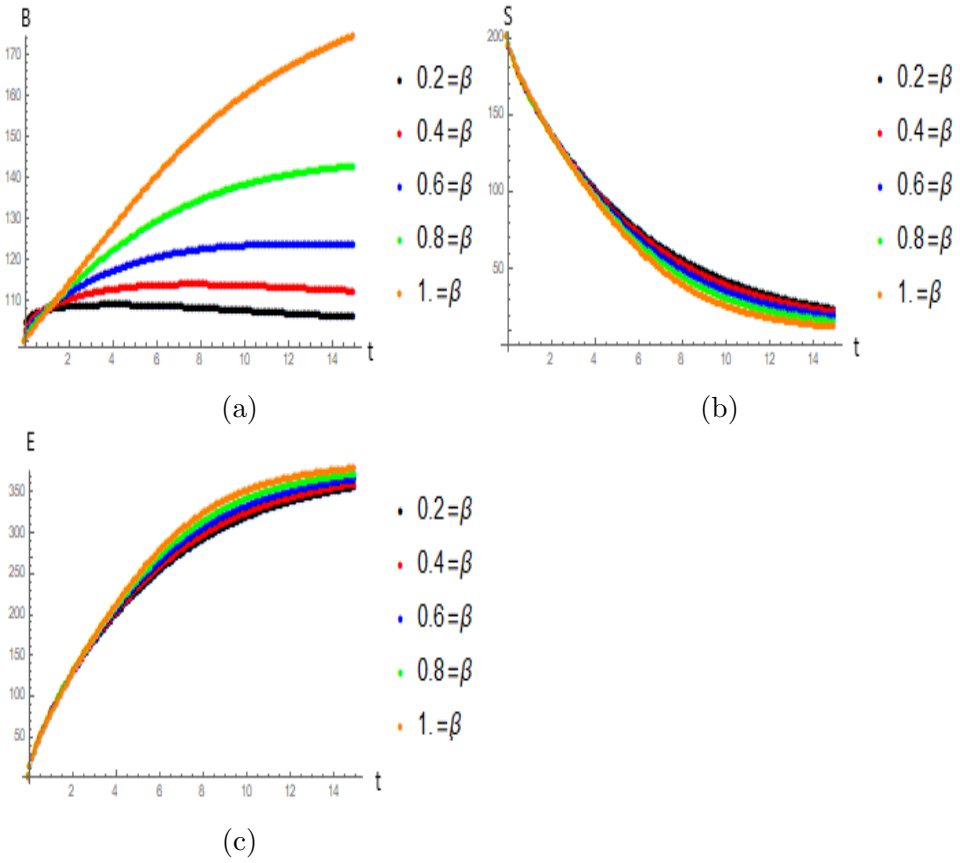

Figure 7: Graphs for the approximate solution B – (a), S – (b) and E – (c). Adams-Bashforth-Moulton method at time step $\tau = 0.1$ is used for Monod model and parameters (23). $\sigma = 0.75$, $\epsilon = 0.75$ and β takes different values in the interval $(0, 1]$.

Figures 6 and 7 represent the numerical results from the **First experiment** for Lotka-Volterra and Monod model, respectively. Here the values of σ and ϵ are fixed at 0.75 and β takes different values in the interval $(0, 1]$ starting from 0.2 with step 0.2. It is seen on the figures that the graphs of S (figures 6b for Lotka-Volterra model and 7b for Monod model) and E (figures 6c for Lotka-Volterra model and 7c for Monod model) remain almost unchanged for the different values of β.

Figures 6a (Lotka-Volterra model) and 7a (Monod model) show that changing β has a significant impact on B. It is clear from the graphs that for lower values of β the values of B at each moment of time are also lower. On figure 7a it is seen that for $\beta = 0.2$ and $\beta = 0.4$ B starts decreasing at a certain moment which confirms the hypothesis that for $\sigma > \beta$ B is not increasing for at least one set of parameters of the model. However, in some specific cases reaching non-monotonicity might take longer time. This happens when the values of σ and β are close to each other but still $\sigma > \beta$. This is more noticeable for Lotka-Volterra model (figure 6a).

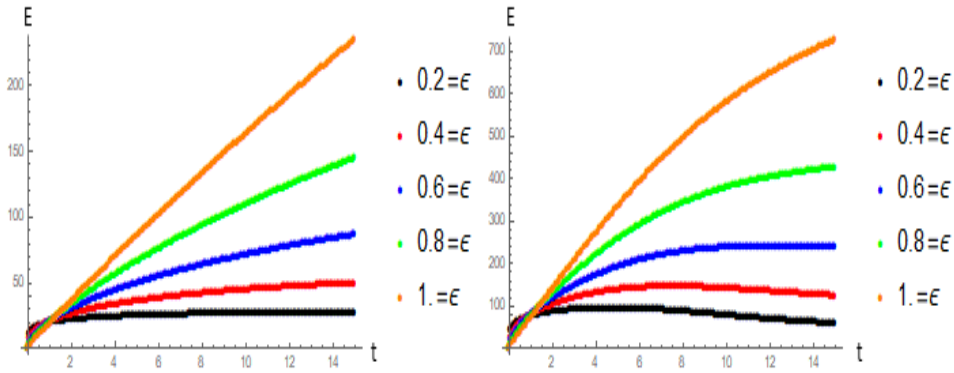

(a) Lotka-Volterra model (b) Monod model

Figure 8: Graphs for the approximate solution E for Lotka-Volterra model with parameters (25) – (a) and Monod model with parameters (23) – (b). Adams-Bashforth-Moulton method at time step $\tau = 0.1$ is used. $\sigma = 0.75$, $\beta = 0.75$ and ϵ takes different values in the interval $(0, 1]$.

The graphs on figure 8 represent the results from the **First experiment** for Lotka-Volterra (figure 8a) and Monod (figure 8b) model. Here the values of σ and β are fixed at 0.75 and the value of ϵ takes different values in the interval $(0, 1]$ starting from 0.2 with step 0.2. Due to the independence of the first two equations on the third one the value of ϵ does not affect the solution for B and S. Therefore only

graphs of E are presented.
Note: *In this case the choice of the values of β and σ satisfies the hypothesis for monotonicity of B.*
The behaviour of E depending on the different values of ϵ is similar to the behaviour of B depending on the different values of β described above: for lower values of ϵ the values of E at each moment of time are also lower. For the Monod model it is seen on the figure 8b that for $\epsilon = 0.2$ and $\epsilon = 0.4$ E starts decreasing at a certain moment which confirms the hypothesis that for $\sigma > \epsilon$ E is not increasing for at least one set of parameters of the model. The fake monotonicity appears again for values of σ and ϵ close to each other but still satisfying $\sigma > \epsilon$ which is more noticeable for Lotka-Volterra model (figure 8a).

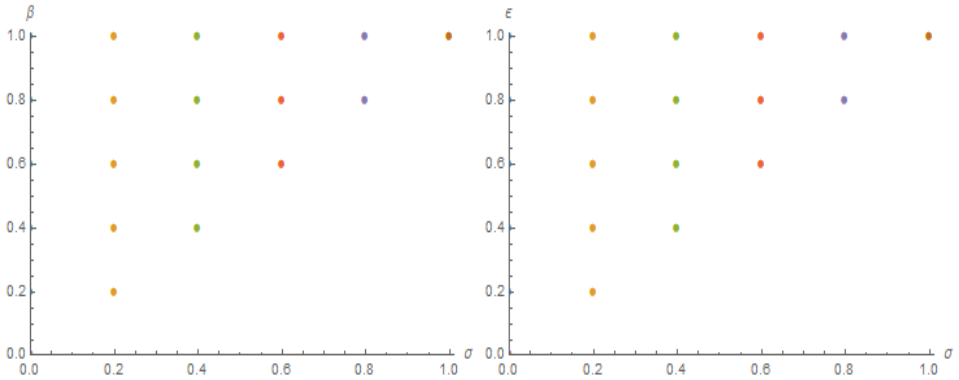

(a) (b)

Figure 9: Numerical results from the **Second experiment** representing the points with coordinates (σ, β) for which B is monotonic – (a) and points with coordinates (σ, ϵ) for which E is monotonic – (b). Monod model with parameters (23) is used.

Figure 9 represents the results form the **Second experiment** for the Monod model and parameters (23).
Figure 9a is a result from the **Second experiment**, method **(a)** and shows the points with coordinates (σ, β) for which B is monotonic. For the numerical calculations σ and β take values in a uniform mesh with step 0.2 on the unit square. It is seen that those coordinates satisfy

$\sigma \leq \beta$ which supports the hypothesis that B is monotonic for $\sigma \leq \beta$ and is not monotonic for $\sigma > \beta$ and at least one set of parameters of the model.
Figure 9b is a result from the **Second experiment**, method **(b)** and shows the points with coordinates (σ, ϵ) for which E is monotonic. For the numerical calculations σ and ϵ take values in a uniform mesh with step 0.2 on the unit square. It is seen that those coordinates satisfy $\sigma \leq \epsilon$ which supports the hypothesis that E is monotonic for $\sigma \leq \epsilon$ and is not monotonic for $\sigma > \epsilon$ and at least one set of parameters of the model.
Note 1: *Method* ***(b)*** *requires solving the whole system (19). Therefore for its implementation a value for β is needed. For obtaining the results shown on figure 9b $\beta = 1$. The choice for the value of β is done according to the hypothesis that for $\sigma \leq \beta$ B is monotonic.*
Note 2: *For most of the points (σ, β) (or (σ, ϵ)) the experiment was performed with $T = 15$. However, in order to avoid fake monotonicity in the cases when $\sigma > \beta$ (or $\sigma > \epsilon$) and their values are close to each other, e.g. $(\sigma, \beta) = (0.4, 0.2)$ (or $(\sigma, \epsilon) = (0.4, 0.2)$) the experiment was performed for a longer period of time.*
Note 3: *The* ***Second experiment****, methods* ***(a)*** *and* ***(b)****, was performed also for Lotka-Volterra model with parameters (25). The corresponding figures are similar to those for the Monod model (figures 9a) and 9b and are not presented here.*

7 Model with included mortality of the biomass

In the previous section 6 the model (19) is studied at the absence of mortality ($m = 0$). Here these investigations are extended, as a term representing mortality of the biomass is added in the model, see the last term in the first equation of (19). The addition of mortality of the biomass implies changes in the behaviour of the solution of the system (7) (more precisely the behaviour of B) in comparison to the case without mortality.

7.1 Properties of the classical model

First, the properties of the classical model ($\beta = \sigma = \epsilon = 1$) will be investigated.
The following system is given:

$$\begin{cases} \frac{db(t)}{dt} = \mu(s(t))b(t) - mb(t),\ 0 < t \leq T \\ \frac{ds(t)}{dt} = -k\mu(s(t))b(t),\ 0 < t \leq T \\ \frac{de(t)}{dt} = p\mu(s(t))b(t),\ 0 < t \leq T \\ b(0) = b_0,\ s(0) = s_0,\ e(0) = e_0 \end{cases} \tag{50}$$

Considering that $\mu(s)$ is function describing specific growth rate, the following properties are required:
- $\mu(s)$ is continuous,
- $\mu(s) > 0, \forall s > 0$,
- $\mu(0) = 0$.

It can be proven that in the case of $m > 0$ **Proposition 1** (for existence and uniqueness) and **Proposition 2** (for positivity) of the solution of (50) formulated in section 4 for $m = 0$ still hold. **Theorem 1** from section 4 also still holds for the functions $s(t)$ and $e(t)$, i.e. $e(t)$ is strictly increasing and $s(t)$ is strictly decreasing in the interval $(0, T)$ (see the proof of **Theorem 1**).
From the posivity of $b(t)$ in the interval $(0, T)$ follows that the sign of $\frac{db(t)}{dt}$ is the same as the sign of $\mu(s(t)) - m$. Hence, $b(t)$ is increasing when $\mu(s(t)) - m > 0$ and decreasing when $\mu(s(t)) - m < 0$ and furthermore, $b(t) \to 0$ as $t \to \infty$. Due to the independence of the first two equations from the system (50) from third one for simplicity of the analysis the following system will be investigated:

$$\begin{cases} \frac{db(t)}{dt} = \mu(s(t))b(t) - mb(t),\ 0 < t \leq T \\ \frac{ds(t)}{dt} = -k\mu(s(t))b(t),\ 0 < t \leq T \\ b(0) = b_0,\ s(0) = s_0. \end{cases} \tag{51}$$

First of all its points of equilibrium are found by solving the system:

$$\begin{cases} \mu(s(t))b(t) - mb(t) = 0 \\ -k\mu(s(t))b(t) = 0. \end{cases} \tag{52}$$

Obviously, each pair $(0, s)$ is a solution. If $b(t) \neq 0$, then system (52) is equivalent to

$$\begin{cases} \mu(s(t)) - m = 0 \\ -k\mu(s(t)) = 0. \end{cases} \tag{53}$$

The latter is incompatible because $m > 0$. Hence, the solutions of (52) are only $(0, s), \forall s \in \mathbf{R}$.
The next step is to evaluate the stability of those equilibrium points. The Jacobi matrix of system (51) has the following form:

$$J(b, s) = \begin{bmatrix} \mu(s) - m & \mu'(s)b \\ -k\mu(s) & -k\mu'(s)b \end{bmatrix}. \tag{54}$$

Then

$$J(0, s) = \begin{bmatrix} \mu(s) - m & 0 \\ -k\mu(s) & 0 \end{bmatrix}. \tag{55}$$

Obviously the eigenvalues of (55) are $\lambda_1 = 0$ and $\lambda_2 = \mu(s) - m$ and therefore $(0, s)$ is a stable equilibrium if $\lambda_2 < 0$, i.e. $\mu(s) - m < 0$. In other words, when mortality prevails over growth, the biomass starts declining to zero. This, of course, totally makes sense from a biological point of view.

7.2 Fractional order derivative model

The next step is to investigate whether the properties obtained for the classical model with mortality of the biomass also hold for fractional values of β and σ in the interval $(0, 1]$. The numerical procedure here is similar to the one that was presented in section 6 for the case without mortality. It consists of the following two experiments:

First experiment: Knowing the behaviour of the solution of (51) depending on the different values of the mortality coefficient m and the initial conditions in the classical case, the purpose of this experiment is to see whether similar conclusions can be made also for the fractional order derivative case. For this experiment the value of β is fixed and σ is taking different values in the interval $(0, 1)$. The system (51) is numerically solved via Adams-Bashforth-Moulton predictor-corrector method. Different values of m are taken such as:
(a) *$\mu(s) - m$ has a solution (changes its sign) in the interval $(0, s_0)$,*
(b) *$\mu(s) - m$ does not have a solution (does not change its sign) in the interval $(0, s_0)$.*
Note 1: *The derivative orders for every experiment for the case in question are chosen in order to satisfy the experimentally established conditions for maintaining monotonicity in the non-mortality case. Briefly, $\beta \geq \sigma$. For the **First experiment** $\beta = 1$ is fixed and σ takes different values in the interval $(0, 1]$. In particular, results for the classical case are also presented.*
Note 2: *If $\mu(s) - m$ does not change its sign in the interval $(0, s_0)$ plus the fact that $s(t)$ is decreasing and hence, takes values only in this interval, means that it is logical to expect that $b(t)$ is monotonic in this case. Furthermore, $\mu(0) = 0$, thus $\mu(0) - m < 0, \forall m > 0$. Finally, if $\mu(s) - m$ does not change its sign in the interval $(0, s_0)$, so $\mu(s) - m < 0$, i.e. $b(t)$ should be decreasing in $(0, T)$.*
Second experiment: In was already commented that in the classical case depending on the value of m and the initial conditions $b(t)$ is either a decreasing function, either increasing until a certain moment in time and then starts to decrease. In each case $b(t)$ is not an increasing function in the whole interval $(0, T)$. The purpose of this experiment is for fixed m to eliminate the values of σ and β in the interval $(0, 1]$ for which the approximate solution B of (51) is increasing in the whole interval $(0, T)$. The algorithm of the experiment is similar to the one described for the **Second experiment** in section 6 for the case without mortality of the biomass. First, the system (51) is solved for given β, σ and m via the Adams-Bashforth-Moulton predictor-corrector method. A counter is set at 0. After the approx-

imate solution (B, S) is calculated, the following check begins: For $j = 0, ..., M - 1$, if $B_{j+1} > B_j$, then the counter increases with 1. The output of the method is boolean, i.e. 0 or 1: if the value of the counter after the check is completed is less than the number of iterations M, then the output is 1 and otherwise it is 0. In other words, if the counter equals M, this means that $B_{j+1} > B_j,\ j = 0, ..., M$, i.e. B is strictly increasing in the set interval $(0, T)$ so the corresponding values of σ and β should be excluded. Graphically the result of a single calculation of the method is represented by a point with coordinates (σ, β) by multiplying those coordinates with the result form the algorithm, i.e. 0 or 1. This way, when different values of σ and β are used for a particular value of m, on the corresponding graph appear only the points whose coordinates (σ, β) are not excluded by the algorithm.

7.3 Numerical results for Monod model

Note 1: *Everywhere in this subsection* s_1 *denotes the solution of* $\mu(s) = m$ *in the interval* $(0, s_0)$.
Note 2: *The values of* σ *and* β *for the numerical calculations are chosen in order to meet the requirements for monotonicity of* B *in the case without mortality of the biomass, i.e.* $\sigma \leq \beta$.

Figure 10 represents the results from the **First experiment** when

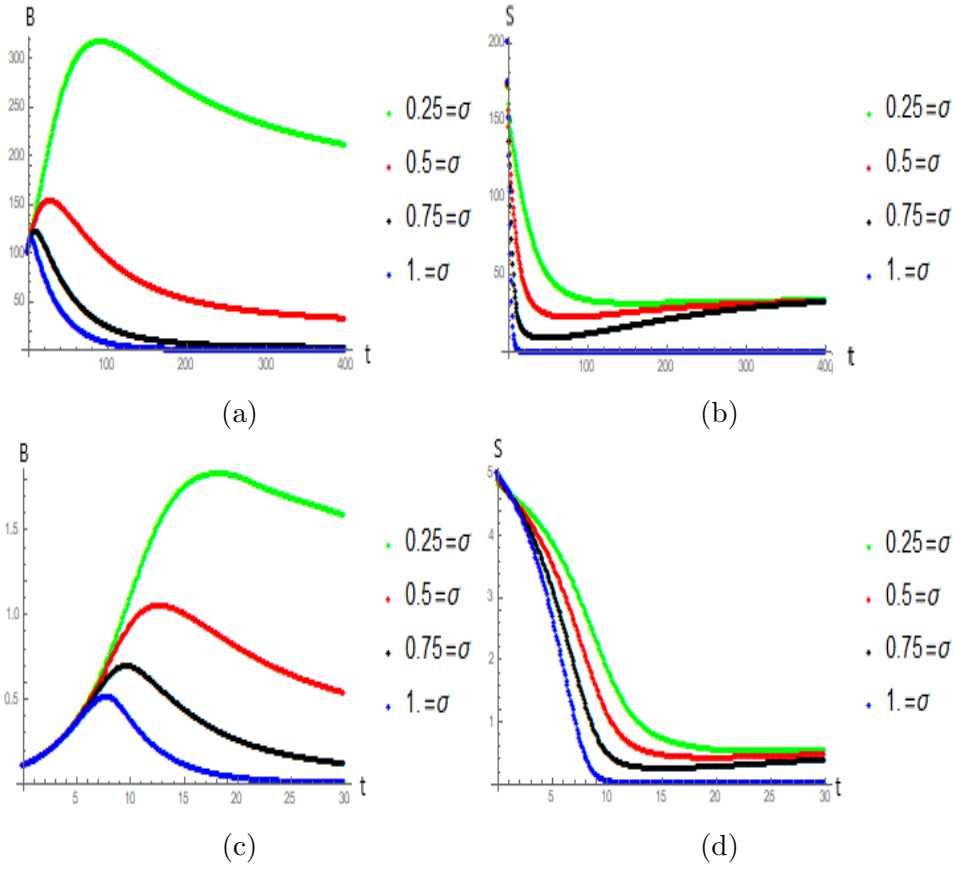

Figure 10: Graph of the approximate solution B (left) and S (right), Monod model, $m = 0.03/0.25$, $s_1 = 34/0.58$, $\beta = 1$, parameters (23)/(24)

the value of m is chosen such that $\mu(s_1) = m$ for $s_1 \in (0, s_0)$. Monod model with parameters (23), $m = 0.03$, $s_1 = 34$ (figures 10a and 10b) and (24), $m = 0.25$, $s_1 = 0.58$ (figures 10c and 10d) is used. The blue graph represents the classical model ($\beta = \sigma = 1$) and the behaviour of its solution meets the expectations for the case when $\mu(s) - m$ changes its sign in the interval $(0, s_0)$: B is increasing until a certain moment $t_1 \in (0, T)$, $s(t_1) = s_1$ and then starts to decrease. S is decreasing and tending to 0. For the fractional values of σ – $\sigma = 0.75, 0.5, 0.25$ the behaviour of B is similar to that in the classical model. However, it is seen on the figures on the left that in the cases when $\sigma < 1$ S starts to increase at a certain moment which is not logical for the process.

Figure 11 represents the results from the **First experiment** when the value of m is chosen such that $\mu(s) - m$ does not change its sign in the interval $(0, s_0)$. Monod model with parameters (23), $m = 0.07$ (figures 11a and 11b) and (24), $m = 0.25$, (figures 11c and 11d) is used. The blue graph represents the classical model ($\beta = \sigma = 1$) and the behaviour of its solution meets the expectations for the case when $\mu(s) - m$ does not change its sign in the interval $(0, s_0)$: B and S are decreasing in the interval $(0, T)$. Like in the previous case, for the fractional values of σ – $\sigma = 0.75, 0.5, 0.25$ the behaviour of B is similar to that in the classical model but in the cases when $\sigma < 1$ S starts to increase at a certain moment which is not logical for the process (it is visible on figure 11b).

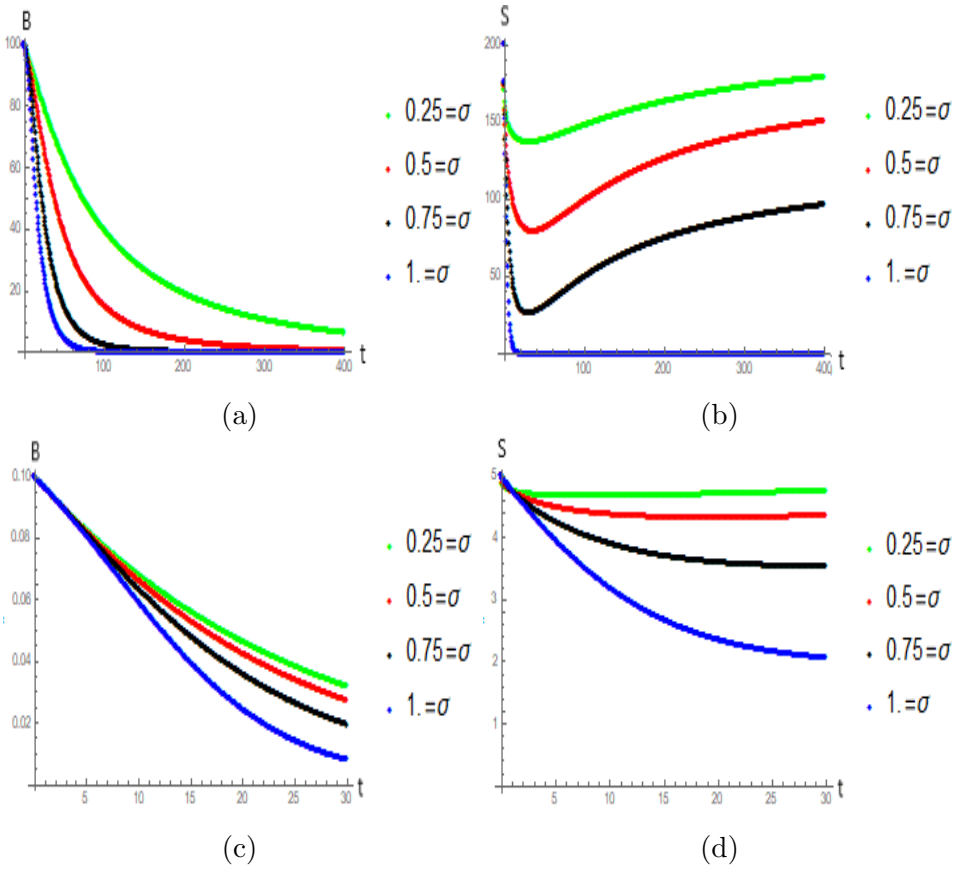

Figure 11: Graph of the approximate solution B (left) and S (right), Monod model, $m = 0.07/0.55$, $\beta = 1$, parameters (23)/(24)

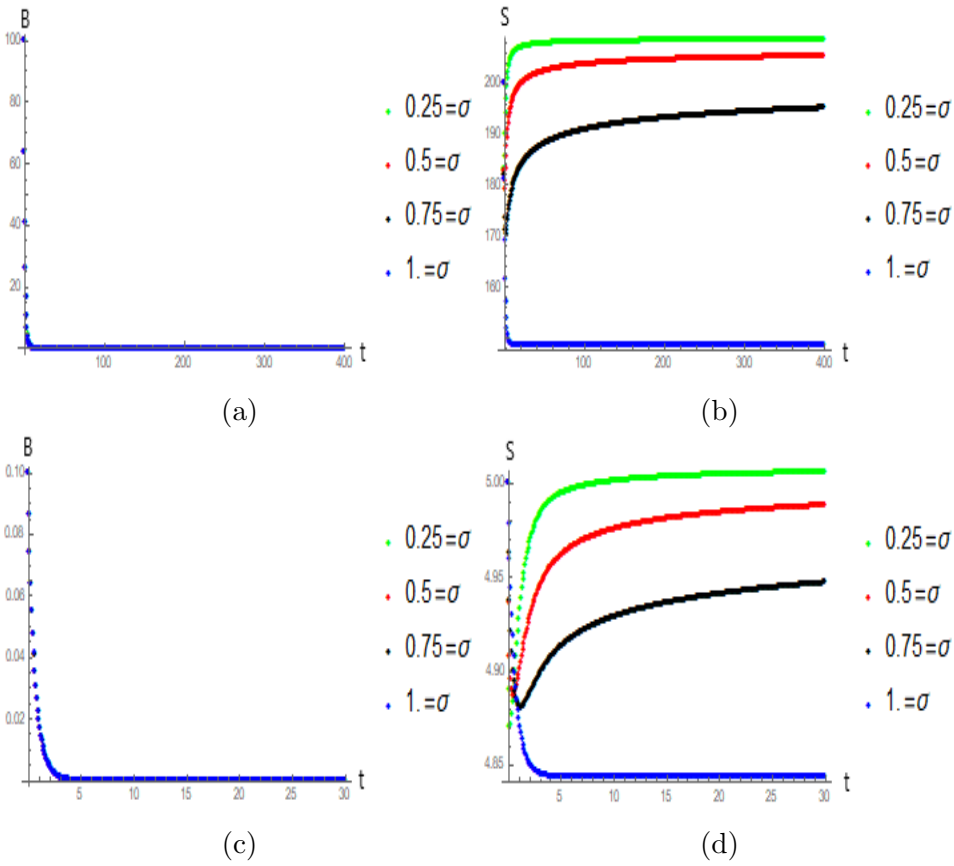

Figure 12: Graph of the approximate solution B (left) and S (right), Monod model, $m = 0.7/2$, $\beta = 1$, parameters (23)/(24)

Figure 12 also represents results from the case when the sign of $\mu(s) - m$ remains unchanged in the interval $(0, T)$ for larger values of m. Monod model with parameters (23), $m = 0.7$ (figures 12a and 12b) and (24), $m = 2$ (figures 12c and 12d) is used. In this case the behaviour of B for the different values of m does not differ from that in the classical case (see figures 12a and 12c). On one hand, this case compared to the previous one shows that the larger the value of m, the faster B is decreasing which is logical considering that m denotes the mortality of the biomass. On the other hand, the illogical increasing

of S for $\sigma < 1$ is even more noticeable for larger values of m.

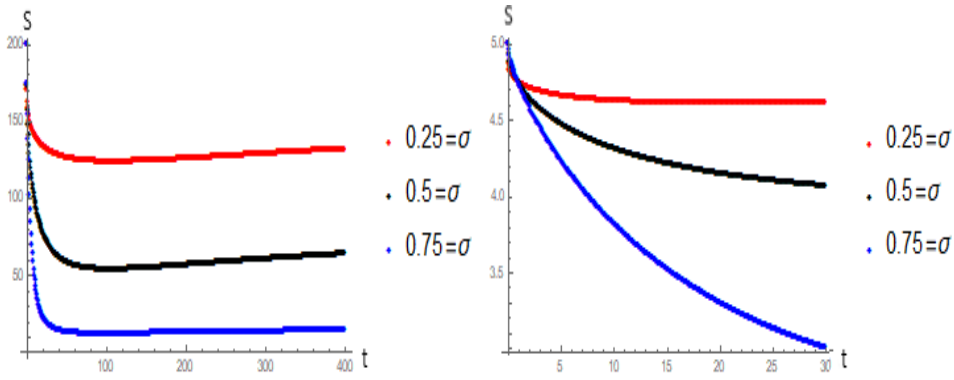

(a) (b)

Figure 13: Graphs of the approximate solution S, Monod model, $\beta = 0.75$, parameters (23), $m = 0.07$ – (a) and (24), $m = 0.55$ – (b)

The results presented so far on figures 10 – 12 show that when mortality of the biomass is included in the model, $\beta = 1$ and $\sigma \in (0, 1)$:
- the behaviour of B follows the logic of the classical model depending on the different values of m which define the sign of $\mu(s) - m$
- in some cases, especially for larger m, when $\sigma < 1$, S is increasing which is not logical for the process.
The following question arises: For which values of β and σ the behaviour of S does not make sense and are there any requirements for those values in order to prevent such kind of behaviour? Although the results presented so far in this section do not provide a clear answer to this question, based on them and additional calculations for $\beta = 0.75$ and $\sigma \in (0, 1)$, $\sigma \leq \beta$ it can be assumed that the illogical behaviour of S appears when $\sigma < \beta$ and does not appear when $\sigma = \beta$. Figures 13 and 14 represent the graphs of S in the case when $\mu(s) - m$ does not change its sign in the interval $(0, s_0)$. It is seen that only when $\sigma = \beta = 0.75$ (the blue graphs) S is decreasing which corresponds to the bioprocess that is being modeled.

Figure 15 represents the result from the **Second experiment** described in this section. The points on the figure represent those (σ, β)

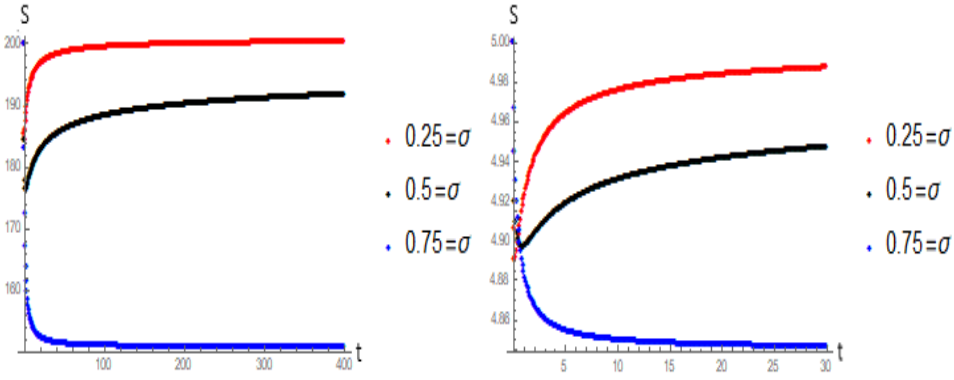

(a) (b)

Figure 14: Graphs of the approximate solution S, Monod model, $\beta = 0.75$, parameters (23), $m = 0.7$ – (a) and (24), $m = 2$ – (b)

for which the solution B of (19) is not increasing in the case when $\mu(s_1) = m$ for some $s_1 \in (0, s_0)$. For the numerical calculations σ and β take values in a uniform mesh with step 0.2 on the part of the unit square where $\sigma \leq \beta$. Every point of this mesh is on the figure which leads to a conclusion that if $\sigma \leq \beta$ B is not increasing in the interval $(0, T)$. The results from this experiment are only primary and show that there is no reason to eliminate any of (σ, β) for which $\sigma \leq \beta$ when it comes to the behaviour of B.

Note: *Only one figure is presented as a result from the* ***Second experiment*** *because for other values of m the figures look the same.*

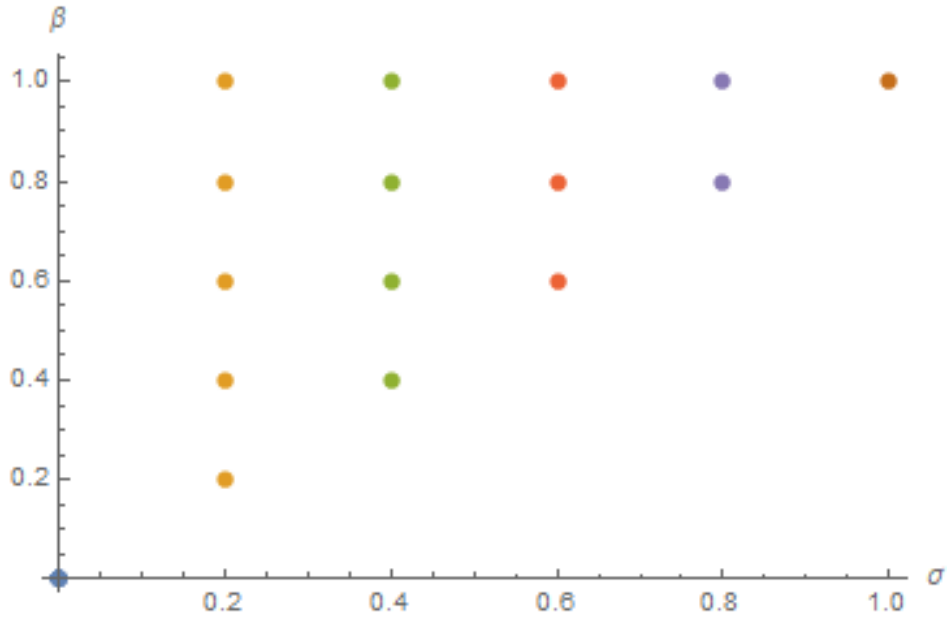

Figure 15: Numerical results from the **Second experiment** representing the points with coordinates (σ, β) for which B is not increasing in the whole interval $(0, T)$. Monod model with parameters (23) is used. $m = 0.05$, $s_1 = 85$

8 Conclusions and future work

This section summarizes the main results from this thesis. At the end, some future development plans on the subject are noted.

Here are the main conclusions from what is done so far:
1. The fractional order derivative models are gaining more and more popularity lately. Recent experiments show that it is more suitable for some processes (mainly biological) to be modeled with a fractional order derivative models. The main reason for this is the quantitative superiority of this type of models – especially for the memory effect which is important for the accuracy of the bioprocesses. There is, however, a serious drawback of using the fractional derivative models, which goes together with the advantages.
2. The negative side of working with fractional models is the lack of an analytical approach to fractional derivatives in general which makes it difficult to determine some essential for the model properties (such as monotonicity, for example). Therefore, it is necessary to study them numerically with appropriately modified numerical methods.
3. For the problem, subject of this work, different scenarios are considered and based on significant number of numerical experiments, some empirical hypotheses are derived:
3.1. Firstly, the behaviour of the (numerical) solution of the model without mortality of the biomass is observed. A comparison between the classical and the fractional derivative model is made. The conclusion is that there exist certain dependencies between the orders of the derivatives for which the classical monotonicity properties remain unchanged:
(a) *For $\sigma \leq \beta$ b is increasing and for $\sigma > \beta$ b is not increasing for at least one set of parameters of the model,*
(b) *For $\sigma \leq \epsilon$ e is increasing and for $\sigma > \epsilon$ e is not increasing for at least one set of parameters of the model.*

3.2. The second main observation concerns the case when mortality of the biomass is included in the model. Adding the mortality

term to the right side of the first equation of the model affects its sign and hence the behaviour of $b(t)$. After the conduction of several experiments, the following conclusion can be done:
The behaviour of the numerical solution B meets the requirements of the classical case for values of β and σ that satisfy the conditions for monotonicity in the classical case (i.e. $\sigma \leq \beta$). However, one can notice that if $\sigma < \beta$, the approximate solution S starts to increase which completely contradicts with the biological point of perspective of the problem. This anomaly is probably due to the inappropriate choice of some of the parameters.

To continue the study of the bioreactor modelling and to extend the obtained first results, the following tasks are yet to be performed:
1. To combine the diffusion and the fractional order derivative model, i.e. to expand the diffusion model for fractional values of β, σ and ϵ in the interval $(0, 1]$ and see if the dependence of the approximate solution E and the diffusion coefficient d remains similar to that in the classical case. An appropriate numerical method is to be chosen for that purpose.
2. To upgrade the results obtained for the mortality-included case in terms of the approximate solution S – the substrate, and try to find out the reason for its non-logical behaviour in particular cases.
3. It is logical that as two separate processes, the microbial growth and the mortality of the bacteria have different fractional evolution. Therefore it is reasonable to consider the system (19) in the following form:

$$\begin{cases} \frac{db(t)}{dt} = D^{1-\beta_1}[\mu(s(t))b(t)] - D^{1-\beta_2}[mb(t)],\ 0 < t \leq T \\ D_*^{\sigma} s(t) = -k\mu(s(t))b(t),\ 0 < t \leq T \\ D_*^{\epsilon} e(t) = p\mu(s(t))b(t),\ 0 < t \leq T \\ b(0) = b_0,\ s(0) = s_0,\ e(0) = 0,\ \beta_1,\ \beta_2,\ \sigma,\ \epsilon \in (0, 1]. \end{cases} \tag{56}$$

Note that now in the first equation the right side is that contains fractional order derivative operators, not the left one, as it is in the

case of (19). Only if $\beta_1 = \beta_2 = \beta$, then

$$\frac{db(t)}{dt} = D^{1-\beta}[\mu(s(t))b(t) - mb(t)] \tag{57}$$

is equivalent to

$$D_*^{\beta} b(t) = \mu(s(t))b(t) - mb(t). \tag{58}$$

The main purpose is to find out how do the different values of β_1 and β_2 affect the behaviour of the approximate solution and are there similarities with the classical model.

References

R. Alt and S. Markov. Theoretical and computational studies of some bioreactor models. *Comput. Math. Appl.*, 64:350–360, 2012.

D. Baleanu, K. Diethelm, E. Scalas, and J. Trujillo. *Fractional Calculus: Models and Numerical Methods*. World Scientific, Singapore, 2012.

S. Bandyopadhyay, R. Chowdhury, C. Bhattacharjee, and S. Pan. Simultaneous production of biosurfactant and ulsd (ultra low sulfur diesel) using rhodococcus sp. in a chemostat. *Fuel*, 113:107–112, 2013.

I. Bazhlekov and E. Bazhlekova. Fractional derivative modeling of bioreaction- diffusion processes. a. *AIP Conference Proceedings*, 2333 art. #060006, 2021.

I. Bazhlekov and E. Bazhlekova. Fractional derivative model for diffusion-controlled adsorption at liquid/liquid interface, b. *AIP Conference Proceedings*, 2048 art. #050012, 2018.

S. Das, R. K. Calay, and R. Chowdhury. Parametric sensitivity of cstbrs for lactobacillus casei: Normalized sensitivity analysis. *ChemEngineering*, 4:41, 2020.

K. Diethelm. Properties of the solutions to "fractionalized" ODE systems, with applications to processes arising in the life sciences. In D. Spasic, N. Grahovac, M. Zigic, M. Rapaic, and T. Atanackovic, editors, *Proc. Internat. Conf. Fractional Differentiation and its Applications 2016, Vol. 1.*, pages 32–44. Faculty of Technical Sciences, Novi Sad, 2016.

K. Diethelm, N. Ford, and A. Freed. A predictor-corrector approach for the numerical solution of fractional differential equations. *Nonlinear Dynam.*, 29:3–22, 2002.

R. Gorenflo and F. Mainardi. Fractional calculus: Integral and differential equations of fractional order. In A. Carpinteri and F. Mainardi, editors, *Fractals and Fractional Calculus in Continuum Mechanics*, pages 223–276. Springer-Verlag, Wien/New York, 1997.

A. Kilbas, H. Srivastava, and J. J. Trujillo. *Theory and Applications of Fractional Differential Equations*. Elsevier, The Netherlands, 2006.

S. Samko, A. Kilbas, and O. Marichev. *Fractional Integrals and Derivatives: Theory and Applications*. Gordon Breach, New York, 1993.

R. Toledo-Hernandez, V. Rico-Ramirez, G. A. Iglesias-Silva, and U. M.Diwekar. A fractional calculus approach to thed ynamic optimization of biological reactive systems. part i: Fractional models for biological reactions. *Chemical Engineering Science*, 117:217–228, 2014.